



## Thick cobalt coatings obtained by electrodeposition

E. GÓMEZ and E. VALLÉS\*

Laboratori de Ciència i Tecnologia Electroquímica dels Materials (LCTEM), Departament Química Física, Facultat de Química, Universitat de Barcelona, Martí i Franquès, 1, E-08028 Barcelona, Spain  
(\*author for correspondence, fax: +34 93 4021231, e-mail: e.valles@qf.ub.es)

Received 16 November 2001; accepted in revised form 26 March 2002

**Key words:** cobalt, electrodeposition, magnetic properties, SEM, XRD

### Abstract

Thick cobalt coatings (10–40  $\mu\text{m}$ ) with a range of morphology and structure were obtained by electrodeposition on both vitreous carbon and copper electrodes. There is a direct relation between the morphology, structure and magnetic properties of cobalt deposits. A chloride medium at pH 4 and low deposition rates favoured the formation of black, ridge-like deposits of hexagonal close packed (h.c.p.) structure with mixed (100) + (110) preferred orientations. In  $\text{CoCl}_2$  at pH 4 at current densities in excess of  $-80 \text{ mA cm}^{-2}$  and in  $\text{CoSO}_4$ , dull grey deposits of h.c.p. (110) structure formed. Sulfate + citrate and chloride + citrate baths at pH 1.5 and very negative current densities promoted the formation of metallic grey deposits with face centred cubic (f.c.c.) structure. Constant saturation magnetization ( $M_s$ ) was obtained for cobalt deposits independently of their structure ( $M_s = 160 \text{ emu g}^{-1}$ ) although the coercive field ( $H_c$ ) of the material varied: h.c.p. (100) > h.c.p. (110) > f.c.c.

### 1. Introduction

Magnetic films have a wide range of applications as data storage devices and sensors. In particular, the magnetic properties of cobalt and its alloys are of special interest in electronic applications [1, 2]. Thin cobalt films have significant properties, such as phase transformation from h.c.p. to f.c.c. and magnetization reversal. Cobalt films can be deposited by physical vapour methods, but these methods produce a mixture of f.c.c. and h.c.p. phases, and it is difficult to obtain single phase h.c.p. or f.c.c. [3–5]. Electrochemical methods are alternatives to molecular beam epitaxy or sputtering because, by changing the electrodeposition conditions, electrodeposition may be used to control the kind of cobalt coatings obtained with the corresponding change in the magnetic properties [6, 7]. Although many studies have provided desirable magnetic properties, most of them involved thin layers, which are not suitable for mechanical applications [8–10].

Some types of micromachined magnetic sensors and actuators require materials with appropriate magnetic properties as well as a thickness in the region of several micrometre. However, attempts to provide deposits with micrometric thickness do not yield any information about magnetic properties [11, 12].

This paper examines how bath composition, solution pH and electrochemical deposition conditions affect the cobalt deposition when thick deposits are obtained. Our aim was to obtain, by electrodeposition, pure cobalt

structure (h.c.p. or f.c.c.) deposits and to correlate the structure, morphology and magnetic properties of the cobalt films thus obtained with their formation conditions. Specifically, interest is focused on the preparation of low coercivity cobalt films for use as soft magnetic materials.

To avoid influence of the additives on the morphology and structure, additive-free baths were tested.

### 2. Experimental details

Electrodeposition was performed in a conventional three-electrode cell under galvanostatic control and employing an EG&G 273 potentiostat/galvanostat. The voltammetric study and stripping experiments were performed using an Autolab with PGSTAT30 equipment and GPES software.

The solutions were freshly prepared using analytical grade chemicals ( $\text{CoSO}_4 \cdot 7\text{H}_2\text{O}$ ,  $\text{CoCl}_2$ ,  $\text{Na}_3\text{C}_6\text{H}_5\text{O}_7 \cdot 2\text{H}_2\text{O}$  and  $\text{H}_3\text{BO}_3$ ), and the water was first double-distilled and then treated with a Millipore Milli Q system. Cobalt was deposited from  $0.5 \text{ mol dm}^{-3}$  chloride and sulfate solutions with and without sodium citrate. The solution pH was fixed at the desired value by adding hydrochloric or sulfuric acid.

Depending on the experiments, the working electrode was a 2 mm diameter vitreous carbon rod electrode (Metrohm), or a 2 mm diameter copper rod (Johnson Matthey 99.99%). The vitreous carbon electrode was

polished to a mirror finish before each experiment using alumina of different grades (3.75 and 1.87  $\mu\text{m}$ ) and cleaned ultrasonically for 2 min in water. The copper electrode was polished before each experiment using diamond (6 and 1  $\mu\text{m}$ ) and alumina (0.3  $\mu\text{m}$ ) suspended in distilled water and cleaned ultrasonically for 2 min in water. The reference electrode was Ag|AgCl|NaCl 1 mol  $\text{dm}^{-3}$  mounted, when necessary, in a Luggin capillary containing 0.5 mol  $\text{dm}^{-3}$   $\text{Na}_2\text{SO}_4$ . All potentials were referred to this electrode. The counter electrode was a platinum spiral.

Deposition was performed at 25 °C. The pH of all solutions was measured before and after deposition. During the deposition the solution was stirred by argon flow. The deposits were examined on a Hitachi 2300 scanning electron microscope.

X-ray diffraction (XRD) phase analysis was performed on a Philips MRD diffractometer using its low-resolution parallel beam optics. The  $\text{CuK}_\alpha$  radiation ( $\lambda = 154, 18 \text{ pm}$ ) monochromatized was selected by means of a diffracted-beam flat graphite crystal.  $2\theta/\theta$  diffractograms were obtained in the  $2\theta = 30\text{--}100^\circ$  range with a step of  $0.05^\circ$  and a measuring time of 5 s per step.

The magnetic measurements were performed with a Manics DSM8 pendulum-type magnetometer at room temperature.

### 3. Results

#### 3.1. Preparation of cobalt deposits

The cobalt deposits were prepared in galvanostatic conditions at current densities between  $-22$  and  $-640 \text{ mA cm}^{-2}$  over both vitreous carbon and copper electrodes. Deposits with thickness ranging from 10 to 40  $\mu\text{m}$  were prepared. The potential–time transients corresponded to a process of nucleation and growth. The curves showed the typical nucleation spike, after which the potential evolved to a quasi-stationary value.

On both substrata the morphology and structure of the final deposits obtained in the same electrodeposition conditions were similar. Thick cobalt deposits were mainly obtained over copper substrate because the adherence was better.

##### 3.1.1. Cobalt deposits obtained from $\text{CoCl}_2$ and $\text{CoSO}_4$ baths

First, cobalt deposits from  $\text{CoCl}_2$  solution at pH 4 were prepared. The structural determination of all deposits by XRD revealed that a h.c.p. phase formed under all conditions. However, the relative predominance of the different orientations depended on the applied current density. At current densities less negative than  $-80 \text{ mA cm}^{-2}$ , coexisted mainly h.c.p. (100) + (110) orientations (Figure 1(a)). By comparing the relative height of the different diffraction peaks, it was observed that h.c.p. (100) was present in a higher proportion than the predicted by the random distribution. At more

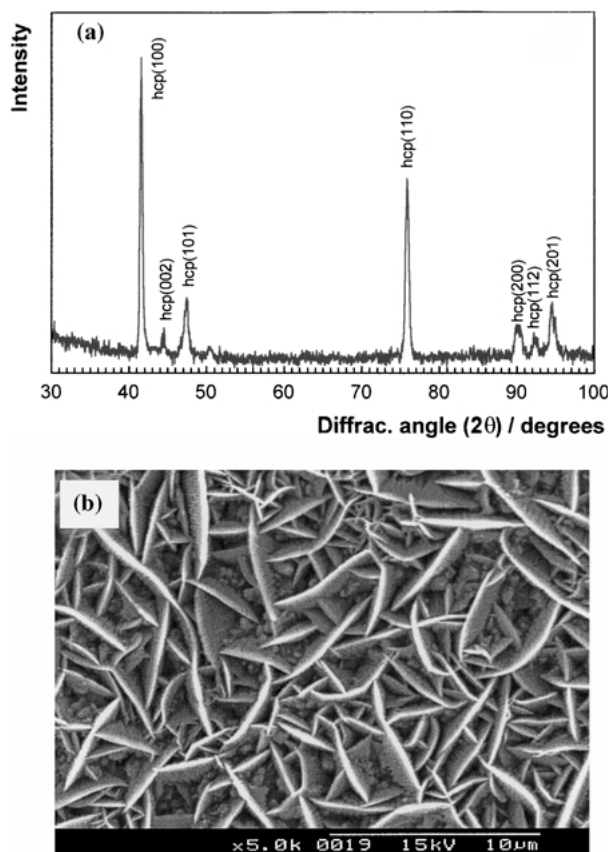


Fig. 1. (a) Diffraction peaks for cobalt deposits obtained at  $-3.2 \text{ mA cm}^{-2}$  from a  $0.5 \text{ mol dm}^{-3}$   $\text{CoCl}_2$ , pH 4 solution. (b) Corresponding SEM micrograph.

negative currents, h.c.p. (110) was the main preferential orientation (Figure 2(a)). This structural change was accompanied by a morphological change: the deposits obtained at low current density showed ridge structure (Figure 1(b)), whereas when the deposits showed the (110) preferential orientation pointed-pyramids (trigonal or tetragonal) were formed (Figure 2(b)), and the edges were smoothed as the applied current density decreased (Figure 2(c)). All deposits were crack-free, even those obtained at very negative current densities.

When cobalt deposits were prepared from this chloride bath at low pH (pH 2.5 and 1.5), they also corresponded to an h.c.p. phase, and for all electrodeposition conditions a (110) preferential orientation was observed and the morphology was pointed-pyramidal. The coatings obtained from these more acidic solutions showed cracks when the deposits were obtained at the more negative current densities.

Similarly, cobalt deposits were obtained from a cobalt sulfate bath in the same pH solutions and electrodeposition conditions as those used for the chloride bath. In contrast to the chloride bath, only cobalt deposits with h.c.p. (110) preferential orientation were obtained. For the deposits obtained at the more negative current densities and especially at low pH, a faint signal corresponding to f.c.c. phase appeared in the diffractogram.

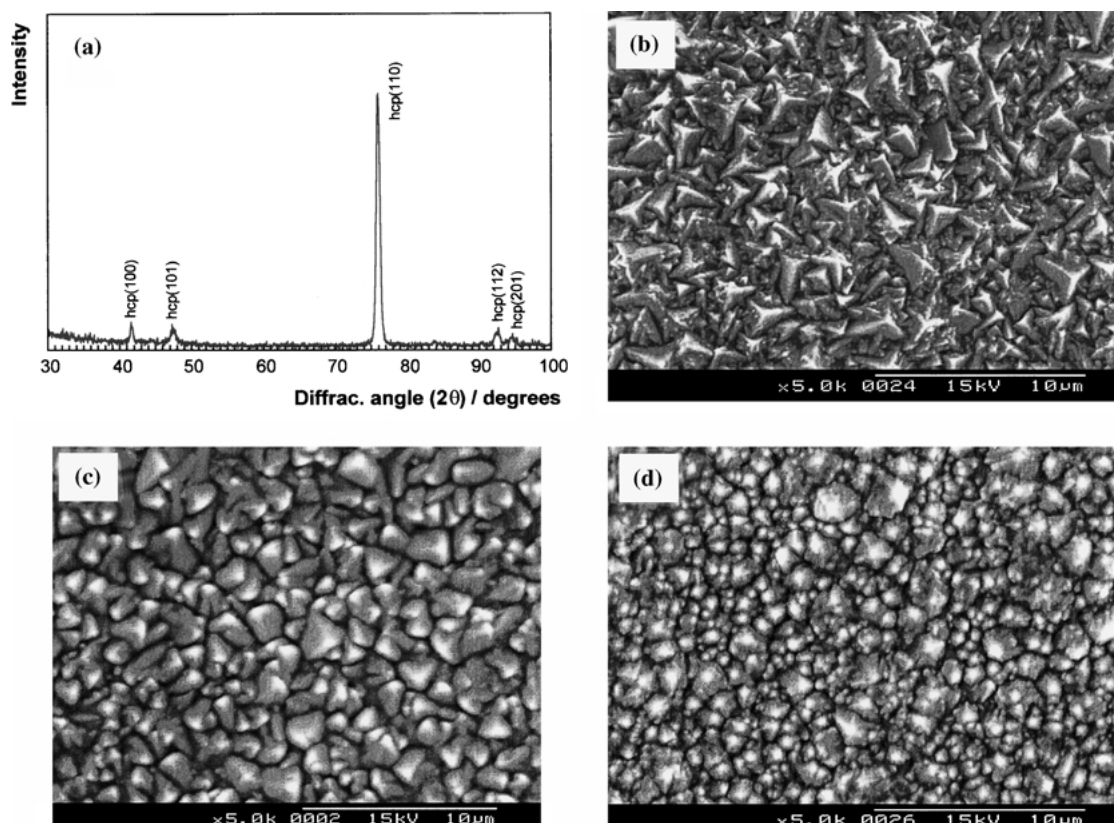


Fig. 2. (a) Diffraction peaks for cobalt deposits obtained at  $-95.5 \text{ mA cm}^{-2}$  from a  $0.5 \text{ mol dm}^{-3}$   $\text{CoCl}_2$ , pH 4 solution. (b) Corresponding SEM micrograph. (c) SEM micrograph for cobalt deposits obtained at  $-318.5 \text{ mA cm}^{-2}$  from a  $0.5 \text{ mol dm}^{-3}$   $\text{CoCl}_2$ , pH 4 solution. (d) SEM micrograph for cobalt deposits obtained at  $-318.5 \text{ mA cm}^{-2}$  from a  $0.5 \text{ mol dm}^{-3}$   $\text{CoSO}_4$ , pH 4 solution.

The stabilization potential value obtained in the galvanostatic transients ( $E_{st}$ ) with the sulfate solution was more negative than that obtained from the chloride bath (Table 1). The difference in characteristic potentials for chloride and sulfate media has been explained on the basis of the different activity coefficients in sulfate and chloride solution [13, 14]. This revealed that, in galvanostatic conditions, the growth of cobalt deposits from sulfate solution took place at more negative potentials and at a lower efficiency than in the chloride due to favoured hydrogen evolution. At lower pH, the deposition took place at even more negative potentials, but the sequence  $E_{st \text{ chloride}} > E_{st \text{ sulfate}}$  was maintained.

The deposit grain size obtained from sulfate bath was smaller than that obtained from a chloride bath in similar conditions (Figure 2(d)), probably due to the

more negative deposition potential required in the sulfate bath to allow the programmed current. In the same way, for fixed electrodeposition conditions, the deposits were more stressed than those obtained from a chloride bath. A detailed observation of the grains also showed a pointed-pyramidal morphology, although at these conditions pentagonal pyramids were observed.

Therefore, both sulfate and chloride baths promoted the formation of deposits of the h.c.p. phase. In most conditions, the deposits corresponded to the (110) preferential orientation, and only when the deposits were prepared from chloride bath at pH 4 and at low rate deposition the (100) preferential orientation was obtained. When the (100) was the preferential orientation pointed-pyramidal morphology was observed, whereas when (100) and (110) were present ridge-like deposits were obtained.

As our objective was to obtain a bath that enabled us to vary the electrodeposition conditions in order to prepare cobalt deposits with either h.c.p. or f.c.c. structure, we tried to modify the bath. To this end, we added sodium citrate at  $0.5 \text{ mol dm}^{-3}$  to the previously studied baths.

### 3.1.2. Chloride + citrate and sulfate + citrate baths

The addition of citrate modified the appearance of the deposits in both cases. At pH 4 and at low negative current, the XRD results indicated that their structure

Table 1. Stabilization potential ( $E_{st}$ ) in the galvanostatic transients obtained at different current densities ( $j$ ) in chloride or sulfate baths at pH 4

$j/\text{mA cm}^{-2}$	$0.5 \text{ mol dm}^{-3} \text{ CoCl}_2$		$0.5 \text{ mol dm}^{-3} \text{ CoSO}_4$	
	$E_{st}/\text{mV}$	Structure	$E_{st}/\text{mV}$	Structure
-3.2	-778	h.c.p. (100)		
-22	-857	h.c.p. (100)	-925	h.c.p. (110)
-96	-975	h.c.p. (110)	-1105	h.c.p. (110)
-319	-1230	h.c.p. (110)	-1580	h.c.p. (110)
-637	-1350	h.c.p. (110)	-1800	h.c.p. (110)

mainly corresponded to the h.c.p. phase, and no preferential orientation was observed. However, in addition to the h.c.p. peaks, other peaks of very low intensity corresponding to f.c.c. appeared in the diffractograms. However, when the deposits were obtained at more negative current densities, the percentage of f.c.c. phase increased. This change of f.c.c. phase was accompanied by a change in the appearance of the deposits.

The deposits obtained at the more negative applied current ( $-637 \text{ mA cm}^{-2}$ ) showed a nodular morphology and the corresponding diffractogram mainly showed peaks corresponding to the f.c.c. structure. At pH 1.5, deposits of just f.c.c. phase took place (Figure 3(a) and 3(b)), and to obtain similar proportion of h.c.p. and f.c.c. phase, it was necessary to apply a less negative current density than that for the solution of pH 4. This means that the addition of citrate favoured the formation of deposits of f.c.c. structure upon decreasing both current density and pH of the solution.

The presence of citrate meant that to achieve the desired current, the stabilization potentials dropped to more negative values. This response corresponded to the complexation of cobalt cations by citric species, as the diminution of free cobalt required more negative potentials. However, when the pH was lowered, the deposition was favoured, because under these more

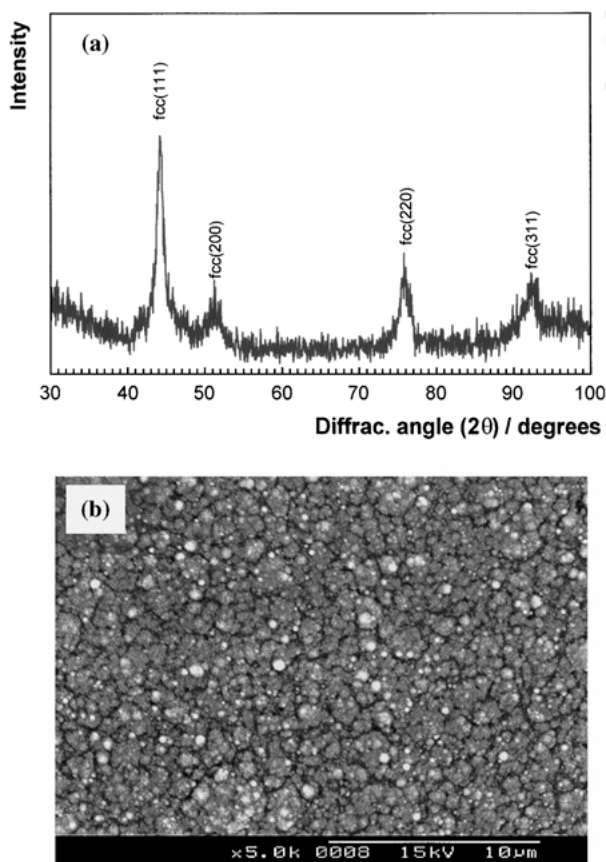


Fig. 3. (a) Diffraction peaks for cobalt deposits obtained at  $-637 \text{ mA cm}^{-2}$  from a  $0.5 \text{ mol dm}^{-3} \text{ CoCl}_2 + 0.5 \text{ mol dm}^{-3} \text{ Na}_3\text{C}_6\text{H}_5\text{O}_7$ , pH 1.5 solution. (b) Corresponding SEM micrograph.

Table 2. Stabilization potential ( $E_{st}$ ) in the galvanostatic transients obtained from different citrate baths at current density  $j = -637 \text{ mA cm}^{-2}$

Bath	pH	$E_{st}/\text{mV}$	Structure
$0.5 \text{ mol dm}^{-3} \text{ CoCl}_2 + 0.5 \text{ mol dm}^{-3} \text{ citrate}$	4	-1720	f.c.c. + some h.c.p.
	1.5	-1300	f.c.c.
$0.5 \text{ mol dm}^{-3} \text{ CoSO}_4 + 0.5 \text{ mol dm}^{-3} \text{ citrate}$	4	-2000	f.c.c. + some h.c.p.
	1.5	-1400	f.c.c.

acidic conditions, the complexation equilibrium was displaced towards citric acid formation, destroying the corresponding citrate-cobalt complex, so that cobalt deposited more readily (Table 2).

The deposits obtained from the cobalt salt + citrate solutions presented more stress than those obtained in the free-citrate bath. This applies especially to the deposits obtained at the more negative currents studied, which showed some cracking and the deposits were poorly adherent to the substrate. However, for fixed conditions, more coherent and less stressed deposits were always obtained from the chloride + citrate bath than from the sulfate + citrate bath.

The presence of boric acid in the salt cobalt + citrate baths was examined at pH 4. Some series of deposits had been prepared at different electrodeposition conditions and no relevant changes were observed with respect to those obtained from the free-boric acid solution.

### 3.2. Magnetic properties of cobalt coatings

From the morphological/structural analysis of the cobalt electrodeposits, three clear kinds of cobalt coatings with defined structure can be obtained in function of the electrolytic bath and the applied current density. The chloride bath, with pH 4 and low negative current densities promoted the formation of black, ridge-like deposits with h.c.p. (100) + (110) structure. At pH 4, both the chloride bath at current densities in excess of  $-80 \text{ mA cm}^{-2}$  and sulfate bath, the formation of dull grey deposits of h.c.p. (110) structure took place. Sulfate + citrate and chloride + citrate baths at pH 1.5 and very negative current densities promoted the formation of metallic grey deposits of f.c.c. structure. For each kind of these three different cobalt deposits, the magnetic properties were examined from magnetization curves measured at room temperature. Two ranges of applied fields were used for each kind of samples, in order to define both saturation magnetization and coercivity of material, which allow our cobalt magnetic materials to be classified. For all cobalt deposits studied, a saturation magnetization of  $160 \text{ emu g}^{-1}$  was observed (Figure 4A) but the coercivity varied for these deposits in the low field range as (Figure 4B)

$$H_c \text{ Co h.c.p. (100) + (110)} > H_c \text{ Co h.c.p. (110)} > H_c \text{ Co f.c.c.}$$

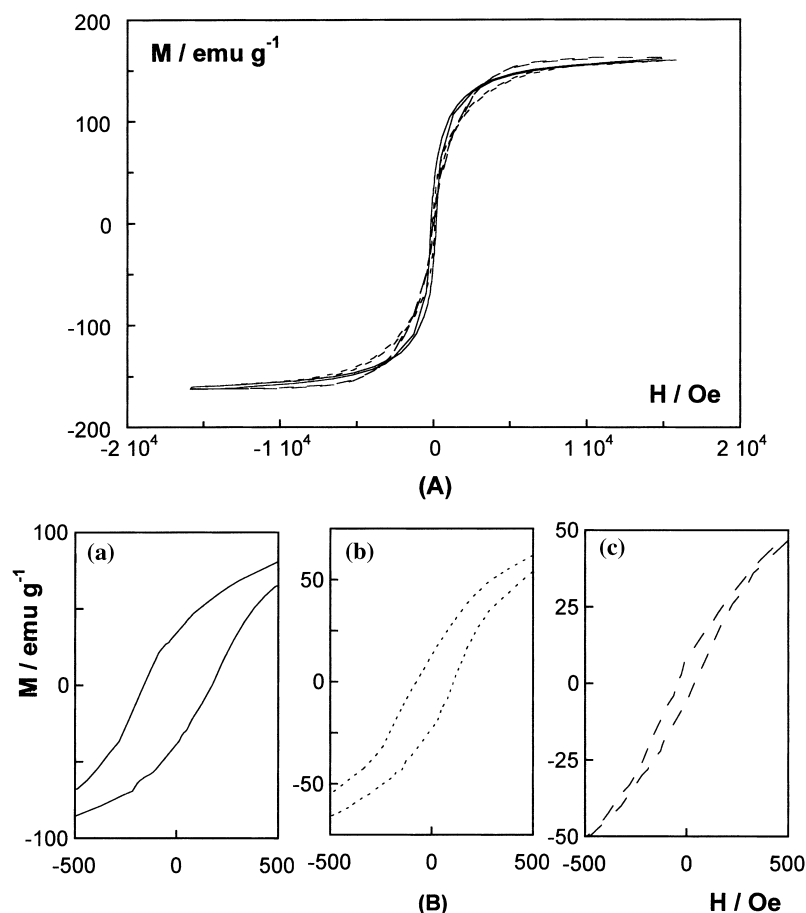


Fig. 4. Magnetic hysteresis curves (A) and magnified details (B) of cobalt deposits obtained from (a)  $0.5 \text{ mol dm}^{-3} \text{ CoCl}_2$ , pH 4 solution at  $-22.3 \text{ mA cm}^{-2}$ . (b)  $0.5 \text{ mol dm}^{-3} \text{ CoCl}_2$ , pH 4 solution at  $-637 \text{ mA cm}^{-2}$ . (c)  $0.5 \text{ mol dm}^{-3} \text{ CoCl}_2 + 0.5 \text{ mol dm}^{-3} \text{ Na}_3\text{C}_6\text{H}_5\text{O}_7$ , pH 1.5 solution at  $-637 \text{ mA cm}^{-2}$ .

### 3.3. Electrochemical study

An electrochemical study was based on three solutions. The solutions were selected according to the kind of deposits obtained: the first was  $\text{CoCl}_2$   $0.5 \text{ mol dm}^{-3}$  at pH 4, which, depending on the electrodeposition conditions, gave a close-hexagonal-packed structure of cobalt with different orientations as a function of the applied current density. The second and third solutions studied were the sulfate + citrate and the chloride + citrate solutions at pH 1.5. These solutions enabled us to obtain f.c.c. phase cobalt deposits independently of the anion, sulfate or chloride content. This study used vitreous carbon electrodes since they did not interfere with the cobalt reduction–oxidation process.

The voltammetric study of the  $\text{CoCl}_2$   $0.5 \text{ mol dm}^{-3}$  showed that the cobalt began to be deposited from around  $-900 \text{ mV}$  (Figure 5A). A high  $Q_{\text{ox}}/Q_{\text{red}}$  ratio, close to 1, was obtained for different negative limits between  $-1000$  and  $-1400 \text{ mV}$ , in both static and stirred conditions. As galvanostatic deposition was mainly used to prepare the deposits, galvanostatic voltammetric curves were also recorded, since this is a good method for testing the efficiency of the galvanostatic deposition. Different current density scans were made to record the potential response. By scanning at low current densities,

high  $Q_{\text{ox}}/Q_{\text{red}}$  ratios were also obtained (Figure 5B), but galvanostatic voltammetric curves showed that the  $Q_{\text{ox}}/Q_{\text{red}}$  ratio decreased when scanning at current densities negative than  $-160 \text{ mA cm}^{-2}$ . This result corroborates the finding that for the preparation of the cobalt h.c.p. with (110) preferred orientation the efficiency was lower than that obtained for the preparation of cobalt h.c.p. with (100) + (110) orientations.

The voltammetric study of cobalt deposition from solutions containing sodium citrate at pH 1.5 showed that in the chloride + citrate solution, the appearance of negative current occurred at potentials more positive than in sulfate + citrate solution (Figure 6A). As can be expected, the  $Q_{\text{ox}}/Q_{\text{red}}$  ratio from these solutions was low with respect to that obtained with  $\text{CoCl}_2$   $0.5 \text{ mol dm}^{-3}$  and pH 4 solution, corresponding to the minor pH value. However, some differences were observed from two solutions, the  $Q_{\text{ox}}/Q_{\text{red}}$  ratio detected in the sulfate + citrate medium was much lower than that observed in chloride + citrate medium (Figure 6B). Similar results were deduced from galvanostatic voltammetric experiments, where it was observed that this difference was maintained even by scanning at the more negative current densities. Although oscillations related to simultaneous hydrogen evolution were seen during the negative scan in both solutions, in the sulfate +

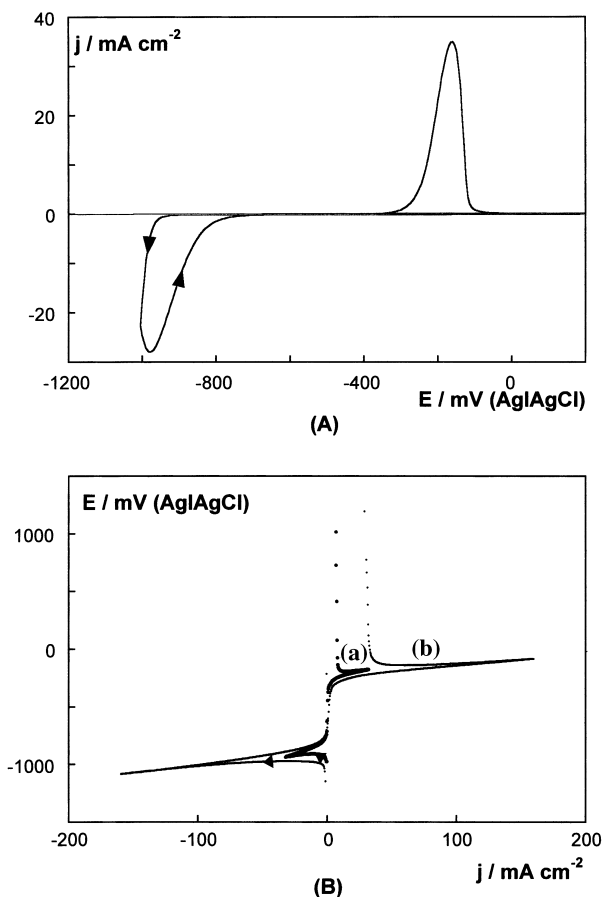


Fig. 5. (A) Cyclic voltammogram at  $\nu = 50 \text{ mV s}^{-1}$  and (B) cyclic galvanostatic voltammograms at (a)  $\nu = 1.6 \text{ mA cm}^{-2} \text{ s}^{-1}$ . Negative limit  $-32 \text{ mA cm}^{-2}$ . (b)  $\nu = 16 \text{ mA cm}^{-2} \text{ s}^{-1}$ . Negative limit  $-160 \text{ mA cm}^{-2}$ . Solution:  $0.5 \text{ mol dm}^{-3} \text{ CoCl}_2$ , pH 4.

citrate bath, the deposition process was less efficient than in the chloride + citrate bath (Figure 6C).

Voltammetric stripping experiments were made for the cobalt deposits obtained at several current densities using the studied solutions. Different solutions were tested in order to oxidize the deposits obtained, blank solutions of  $\text{NaCl } 1 \text{ mol dm}^{-3}$  and  $\text{Na}_2\text{SO}_4 \text{ } 0.5 \text{ mol dm}^{-3}$  or the own deposition solution. The oxidation scan was made at  $10 \text{ mV s}^{-1}$ , and when the deposition bath was used as stripping solution, the scan was always started at a potential at which no deposition occurred.

In all cases, only one oxidation peak was obtained, the position of which was independent of the current density applied during the deposition. Using  $\text{NaCl } 1 \text{ mol dm}^{-3}$  or  $\text{Na}_2\text{SO}_4 \text{ } 0.5 \text{ mol dm}^{-3}$  as the stripping media the deposits oxidized practically at the same potential, whereas when stripping was made in the deposition solution, the oxidation peak appeared at more negative potentials. Therefore, the position of the stripping peaks did not reveal the different morphology and structure of cobalt deposits when current density was gradually decreased or deposition solution changed. Stripping oxidation peaks of f.c.c. cobalt precursor layers were recorded at similar potentials to those of the h.c.p. phase

(Figure 7), revealing that stripping technique does not detect the differing structures of cobalt deposits.

#### 4. Discussion and conclusions

Electrochemical deposition is a good method for monitoring the kind of cobalt deposit obtained, the choice of both the electrolytic solution and the applied current density/potential allowed us to prepare cobalt coatings with a defined morphology, structure and magnetic properties. Although the stable form of cobalt at room temperature is the h.c.p. phase, thick cobalt deposits with mixed h.c.p. + f.c.c. or even f.c.c. structure can be obtained by suitable selection of the bath and/or the electrodeposition conditions. There is a direct relation between morphology, structure and magnetic properties of cobalt deposits, and so observation of the morphology is useful for predicting the kind of structure obtained and hence the expected coating coercivity.

A constant saturation magnetization value was obtained for all the prepared cobalt deposits, irrespective of their structure. The  $M_s$  value ( $160 \text{ emu g}^{-1}$  or  $1425 \text{ kA m}^{-1}$ ) is practically that of bulk cobalt, which corresponds to the formation of thick deposits. This value is greater than that observed by other authors for thin cobalt deposits obtained either by electrodeposition [6] or by sputtering [4] since they prepared thin layers which do not correspond to bulk cobalt. However, for each one of the types of cobalt deposits, we found differing coercivity values as a function of their cobalt morphology and structure as corresponds to a very structure and morphology-sensitive magnitude. Deposits of f.c.c. phase show the lowest coercive field observed.

The use of simple baths always led to deposits of h.c.p. structure with preferred orientation that show characteristic morphology for each orientation.

A chloride medium at pH 4 and low deposition rates favours the formation of ridge-like deposits of h.c.p. (100) + (110) structure, for which a high  $Q_{\text{ox}}/Q_{\text{red}}$  ratio is observed. Therefore, slow growth of the deposit and low hydrogen evolution seems to be suitable for obtaining deposits of h.c.p. phase containing a high percentage of the (100) orientation. The increase of the deposition rate in the chloride bath or the use of sulfate bath favour the formation of pyramidal h.c.p. (110) structure over a wide range of pH values (1.5 to 4). In these conditions, the  $Q_{\text{ox}}/Q_{\text{red}}$  ratio decreases, revealing that simultaneous hydrogen evolution might favour the (110) preferred orientation of the h.c.p. phase. However, the addition of citrate to the chloride or sulfate baths leads to the formation of deposits with f.c.c. structure. The first effect observed due to the presence of citric species in solution is the loss of the preferred orientation. The f.c.c./h.c.p. ratio in the deposits increases, either through the decrease of the deposition potential/current density, at fixed pH, or by the decrease of the pH solution. Therefore, to prepare a nodular f.c.c. structure

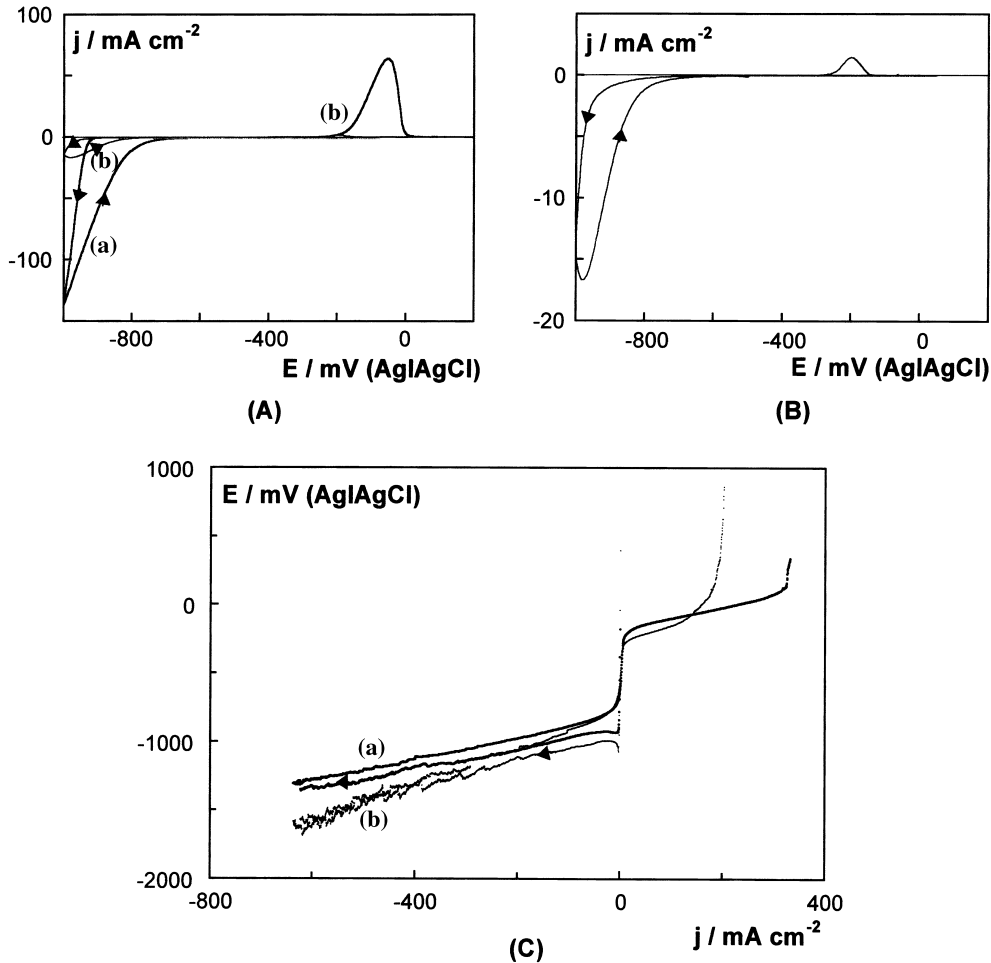


Fig. 6. (A) Cyclic voltammograms at  $\nu = 50 \text{ mV s}^{-1}$  of: (a)  $0.5 \text{ mol dm}^{-3} \text{ CoCl}_2 + 0.5 \text{ mol dm}^{-3} \text{ Na}_3\text{C}_6\text{H}_5\text{O}_7$ , pH 1.5, (b)  $0.5 \text{ mol dm}^{-3} \text{ CoSO}_4 + 0.5 \text{ mol dm}^{-3} \text{ Na}_3\text{C}_6\text{H}_5\text{O}_7$ , pH 1.5. (B) Magnified curve (b) of Figure 6A. (C) Cyclic galvanostatic voltammograms at  $\nu = 16 \text{ mA cm}^{-2} \text{ s}^{-1}$  of (a)  $0.5 \text{ mol dm}^{-3} \text{ CoCl}_2 + 0.5 \text{ mol dm}^{-3} \text{ Na}_3\text{C}_6\text{H}_5\text{O}_7$ , pH 1.5, (b)  $0.5 \text{ mol dm}^{-3} \text{ CoSO}_4 + 0.5 \text{ mol dm}^{-3} \text{ Na}_3\text{C}_6\text{H}_5\text{O}_7$ , pH 1.5.

the optimal conditions are both a low pH solution value and high deposition rate (very negative current densities applied). It seems that citric species favour the growth of cobalt deposit in f.c.c. structure. Moreover, under these

experimental conditions, low efficiency of the deposition process is observed, especially in the sulfate + citrate bath.

From the acidity constants of citric acid [15], different species are predominant in solution at differing pH values and in the absence of cobalt salts. At pH 4,  $\text{H}_2\text{Cit}^-$  is the main species whereas at pH 1.5 the citrate is mainly in the form of citric acid ( $\text{H}_3\text{Cit}$ ). This relative presence of citric species changes when cobalt salt is present in solution, different cobalt–citrate complexes can form [12] ( $\text{CoH}_2\text{Cit}^+$ ,  $\text{CoHCit}$ ,  $\text{CoCit}^-$ ), the dominance of which is dependent on both the solution pH and the complexation constants. At moderate pH values (around 4) cobalt forms complexes with citric species and  $\text{CoHCit}$  and  $\text{CoCit}^-$  exist, being  $\text{CoCit}^-$  the predominant form. For an initial  $\text{Co(II)}$  concentration of  $0.5 \text{ mol dm}^{-3}$ ,  $[\text{CoCit}^-] = 0.327 \text{ mol dm}^{-3}$  and  $[\text{CoHCit}] = 0.127 \text{ mol dm}^{-3}$ .

The cobalt deposit formation occurs, at pH 4, mainly from the reduction of these species.

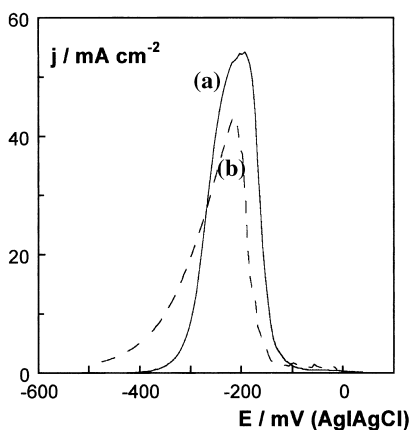
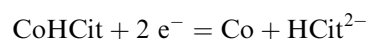
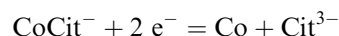
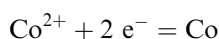


Fig. 7. Stripping voltammograms in  $\text{NaCl } 1 \text{ mol dm}^{-3}$  solution of cobalt deposits obtained at  $-318 \text{ mA cm}^{-2}$  from: (a)  $0.5 \text{ mol dm}^{-3} \text{ CoCl}_2$  pH 4 solution and (b)  $0.5 \text{ mol dm}^{-3} \text{ CoCl}_2 + 0.5 \text{ mol dm}^{-3} \text{ Na}_3\text{C}_6\text{H}_5\text{O}_7$ , pH = 1.5 solution.



whereas, at pH 1.5, complexation is not favoured. The calculated concentration of free cobalt ions reveals that the cobalt present in solution is mainly as the  $\text{Co}^{2+}$  form,  $[\text{Co}^{2+}] = 0.499 \text{ mol dm}^{-3}$ . With respect to the total concentration of citric species ( $0.5 \text{ mol dm}^{-3}$ ), the main form is citric acid, with a calculated concentration of  $0.489 \text{ mol dm}^{-3}$ . Therefore, in pH 1.5 solutions, direct cobalt reduction takes place by:



In citrate media at different pH values, although the formation of cobalt coatings occurs through the reduction of different cobalt species, a percentage of f.c.c. structure is always obtained. Therefore, it is clear that the presence of citric species in solution during the deposition process promotes the formation of f.c.c. cobalt structure, because the reduction of the free cobalt ion in the absence of citrate always leads to the formation of a h.c.p. structure. This effect is probably related to the adsorption of the various citric species, which are predominant at each solution pH, on the deposit during the growth of the cobalt coating. At pH 1.5 the direct adsorption of  $\text{H}_3\text{Cit}$  might occur, whereas at pH 4, the  $\text{Cit}^{3-}$  or  $\text{HCitr}^{2-}$  ions, released during the reduction process, remain adsorbed on the growing deposit, in both cases favouring the formation of the f.c.c. cobalt phase.

Although the h.c.p. structure is the most stable form at room temperature, electrodeposition can produce f.c.c. cobalt coatings with low coercivity values. For this reason, it is necessary to use a complexing/adding agent, such as citrate, to retard h.c.p. cobalt formation. Also, significant hydrogen evolution, which is simultaneous with fast growth of the deposit seems to favour the formation of the less stable form of cobalt, but this process is not sufficient to promote f.c.c. formation.

The low coercivity value observed in the cobalt coatings that present f.c.c. structure obtained from the citrate bath can be related to their small grain size, smaller than that observed for cobalt coatings obtained at similar current densities, from baths without citrate salts. This decreased grain size could be related to the

adsorption process of citric species, and/or to simultaneous hydrogen evolution. The conjunction of these factors produces grain size reduction, which favours the lowering of the coercive field values.

### Acknowledgements

The authors would like to thank the Serveis Científicotècnics (Universitat de Barcelona) for making equipment available. This paper was supported financially by contract MAT 2000-0986 from the Comisión Interministerial de Ciencia y Tecnología (CICYT) and by the Comissionat of the Generalitat de Catalunya under Research Project SGR 2000-017.

### References

1. T. Osaka, *Electrochim. Acta* **45** (2000) 3311.
2. R.M. Bozorth, 'Ferromagnetism' (IEEE Press, 1993, Piscataway NJ).
3. O. Kitakami, H. Sato, Y. Shimada, F. Sato and M. Tanaka, *Phys. Rev. B* **56** (1997) 13849.
4. O. Kohmoto, H. Kitamura, T. Tsuda and F. Ono, *Phys. Stat. Sol.* **176** (1999) 1039.
5. M. Zheng, J. Shen, J. Barthel, P. Ohresser, Ch.V. Mohan and J. Kirschner, *J. Phys. Condens. Matter.* **12** (2000) 783.
6. J.L. Bubendorff, E. Beaurepaire, C. Meny and J.P. Bucher, *J. Appl. Phys.* **83** (1998) 7043.
7. M. Cerisier, K. Attenborough, J.P. Celis and C. van Haesendonck, *Appl. Surf. Science* **166** (2000) 154.
8. V. Scarani, B. Doudin and J.P. Ansermet, *J. Magn. Mag. Mat.* **205** (1999) 241.
9. J.L. Bubendorff, C. Meny, E. Beaurepaire, P. Panissod and J.P. Bucher, *Eur. Phys. J., B* **17** (2000) 635.
10. M. Kleinert, H.F. Waibel, G.E. Engelmann, H. Martin and D.M. Kolb, *Electrochim. Acta* **46** (2001) 3129.
11. J. Scoyer and R. Winand, *Surf. Technol.* **5** (1977) 169.
12. S.S. El Rehim, S.M. El Wahaab, M.A.M. Ibrahim and M.M. Dankeria, *J. Chem. Technol. Biotechnol.* **73** (1998) 369.
13. J. Yeager, J.P. Celis and E. Yeager, *J. Electrochem. Soc.* **106** (1959) 328.
14. I. Epelboin, M. Jusselin and R. Wiart, *J. Electroanal. Chem.* **119** (1981) 61.
15. D.R. Lide (Ed.), 'Handbook of Chemistry and Physics', 77th edn (CRC Press, 1996–1997, New York), pp. 8–50.